

# Lawrence Berkeley National Laboratory

## Lawrence Berkeley National Laboratory

### Title

Introduction of Nonlinear Properties Into Hierarchical Models of Nb<sub>3</sub>Sn Strands

### Permalink

<https://escholarship.org/uc/item/9k75d2td>

### Author

Collins, B.

### Publication Date

2012-05-18

Peer reviewed

Introduction of Nonlinear Properties Into Hierarchical Models of Nb<sub>3</sub>Sn Strands

**B. Collins, J. Krishnan, D. Arbelaez, P. Ferracin, S. O. Prestemon, A. Godeke, D. R. Dieterich, and T. I. Zohdi**

Accelerator Fusion Research Division  
Ernest Orlando Lawrence Berkeley National Laboratory  
University of California  
Berkeley, California 94720

DISCLAIMER

This document was prepared as an account of work sponsored by the United States Government. While this document is believed to contain correct information, neither the United States Government nor any agency thereof, nor The Regents of the University of California, nor any of their employees, makes any warranty, express or implied, or assumes any legal responsibility for the accuracy, completeness, or usefulness of any information, apparatus, product, or process disclosed, or represents that its use would not infringe privately owned rights. Reference herein to any specific commercial product, process, or service by its trade name, trademark, manufacturer, or otherwise, does not necessarily constitute or imply its endorsement, recommendation, or favoring by the United States Government or any agency thereof, or The Regents of the University of California. The views and opinions of authors expressed herein do not necessarily state or reflect those of the United States Government or any agency thereof or The Regents of the University of California.

This work was supported by the Director, Office of Science, Office of Fusion Energy Sciences, of the U.S. Department of Energy under Contract No. DE-AC02-05CH11231.

# Introduction of Nonlinear Properties Into Hierarchical Models of Nb<sub>3</sub>Sn Strands

B. Collins, J. Krishnan, D. Arbelaez, P. Ferracin, S. O. Prestemon, A. Godeke, D. R. Dietderich, and T. I. Zohdi

**Abstract**—The development of computational models representing Rutherford cable formation and deformation is necessary to investigate the strain state in the superconducting filaments in Nb<sub>3</sub>Sn magnets. The wide variety of length scales within accelerator magnets suggests usage of a hierarchical structure within the model. As part of an ongoing investigation at LBNL, a three-dimensional simplified nonlinear multiscale model is developed as a way to extend previous linear elastic versions. The inclusion of plasticity models into the problem formulation allows an improved representation of strand behavior compared to the linear elastic model. This formulation is applied to a single Nb<sub>3</sub>Sn strand to find its effective properties as well as the strain state in the conductor under loading.

**Index Terms**—Elasto-plastic, multiscale modeling, Nb<sub>3</sub>Sn, superconducting magnets.

## I. INTRODUCTION

THE ABILITY to obtain a three dimensional strain state in Nb<sub>3</sub>Sn filaments due to macro-scale loading is vital in determining the critical current carrying capacity of a magnet. However, this task is not trivial due to the variety of important length scales present in superconducting magnets: magnet, coil, cable, strand, filaments, and lattice. Each scale, shown in detail in Fig. 1, plays an important role in the final strain state present in the filaments. Direct numerical simulation of the macro-scale magnet with the inclusion of all the micro-scale details is computationally infeasible. Therefore, multi-scale computation can be used to understand the behavior across various length scales. At Lawrence Berkeley National Laboratory (LBNL), the development of such hierarchical models has begun in order to bridge the entire range of scales present in superconducting accelerator magnets. Due to the vast difference in these length scales, multiple models must be created to accurately incorporate the physics present at each scale. In the present work, the main focus is on the development of models that bridge the strand and filament scales in a rod restack process (RRP) strand.

The numerical determination of the strain state in Nb<sub>3</sub>Sn filaments has been explored previously by multiple researchers. Mitchell [1] has previously developed one and two-dimensional

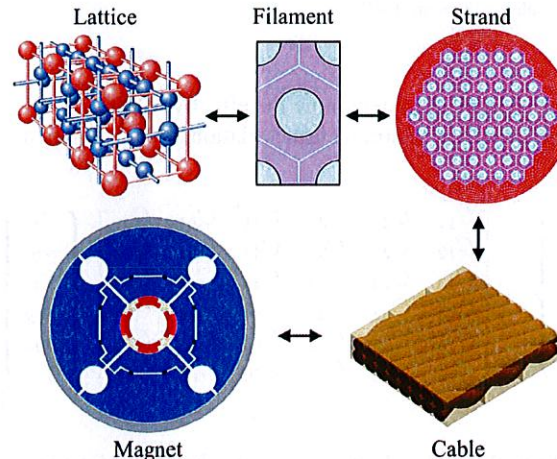


Fig. 1. Illustration of the scales present in Nb<sub>3</sub>Sn magnets: magnet, cable, strand, filaments, lattice.

models to simulate thermo-mechanical loads on a strand and to determine the strain state in Nb<sub>3</sub>Sn filaments. Boso [2], [3] has developed a multi-scale model to simulate Nb<sub>3</sub>Sn conductors. Arbelaez [4] has created a hierarchical scheme to simulate the relationship between the strand and Rutherford cable levels and to determine the effective linear, orthotropic, properties of cables.

In the present study, a computational model is used to examine the behavior between the strand and filament levels. As an extension to the previous linear multi-scale scheme developed by Arbelaez, nonlinear effects are included. In this model, the strand is treated as the macro-scale, with the Nb<sub>3</sub>Sn filaments composing the micro-scale. As an initial step, a cooldown of the strand from 300 K to 4.2 K is examined.

## II. MULTI-SCALE MODELING

### A. Linear Regime

Consider a heterogeneous material with two length scales, shown in Fig. 2, such that  $H \gg h$ . Rather than describing every detail of the microstructure at every location in the macro problem, the problem is separated into two scales: the macro-scale and a Representative Volume Element (RVE), which characterizes the micro-scale. The desired goal is to determine the stress and strain distribution in the micro-scale given a loading condition from the macro-scale.

To approach this goal, a multi-scale model is proposed as follows:

- 1) Compute the effective properties of the RVE. In order to compute these properties, six different loading conditions

Manuscript received August 03, 2010; accepted October 17, 2010. Date of publication December 03, 2010; date of current version May 27, 2011. This work was supported in part by the Director, Office of Science, High Energy Physics, U.S. Department of Energy under Contract DE-AC02-05CH11231.

B. Collins, J. Krishnan, and T. I. Zohdi are with the Lawrence Berkeley National Laboratory, Berkeley, CA 94720 USA, and also with the University of California, Berkeley, CA 94720 USA (e-mail: BCollins@lbl.gov).

D. Arbelaez, P. Ferracin, S. O. Prestemon, A. Godeke, and D. R. Dietderich are with the Lawrence Berkeley National Laboratory, Berkeley, CA 94720 USA.

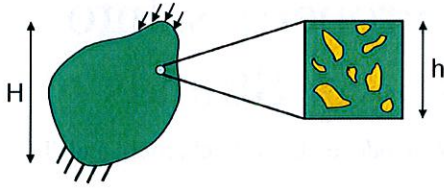


Fig. 2. Illustration of a heterogeneous body being approximated by a Representative Volume Element (RVE).

can be applied to determine the effective elasticity tensor. The linear stress-strain elastic relation can be written as

$$\begin{Bmatrix} \sigma_x \\ \sigma_y \\ \sigma_z \\ \tau_{xy} \\ \tau_{yz} \\ \tau_{zx} \end{Bmatrix} = \begin{bmatrix} C_{11} & C_{21} & C_{31} & C_{41} & C_{51} & C_{61} \\ C_{12} & C_{22} & C_{32} & C_{42} & C_{52} & C_{62} \\ C_{13} & C_{23} & C_{33} & C_{43} & C_{53} & C_{63} \\ C_{14} & C_{24} & C_{34} & C_{44} & C_{54} & C_{64} \\ C_{15} & C_{25} & C_{35} & C_{45} & C_{55} & C_{65} \\ C_{16} & C_{26} & C_{36} & C_{46} & C_{56} & C_{66} \end{bmatrix} \begin{Bmatrix} \varepsilon_x \\ \varepsilon_y \\ \varepsilon_z \\ \gamma_{xy} \\ \gamma_{yz} \\ \gamma_{zx} \end{Bmatrix} \quad (1)$$

where the left column represents the three-dimensional stress state of a material point, the right column represents the strain state of a material point, and an elasticity tensor with thirty six constants connects the two. It can be seen that if only one non-zero value of the strain components is imposed, computation of the stress state will determine the corresponding column of the elasticity tensor. To extract the effective properties of the RVE, six different average strain states over the domain are imposed, and the corresponding average stress states are calculated to construct the effective elasticity tensor. Note that for the linear case the properties of the RVE only need to be determined once since the material behavior is independent of the stress and strain state.

- 2) Use the effective properties of the RVE to solve the macro-scale model.
- 3) Apply resulting stress state to RVE to compute the stress distribution present in the micro-scale.

### B. Nonlinear Regime

When considering nonlinear multi-scale models, the material behavior at a point is dependent on its corresponding stress and strain (or strain increment) states. In order to account for this behavior in the hierarchical model, the effective properties of the RVE can be determined point-wise at the current stress and strain state. In the current model, the effective properties are not actually calculated. Instead, the deforming body is updated according to its elasto-plastic constitutive behavior. Performing a finite element analysis at every material point in the body can be computationally expensive; therefore, material points with near equal stress states are approximated by a single RVE.

In addition, the nonlinear case must be solved incrementally, whereas the solution to the linear problem can be found in a single step.

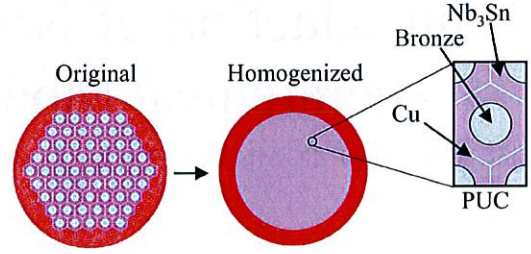


Fig. 3. Homogenization of a RRP strand.

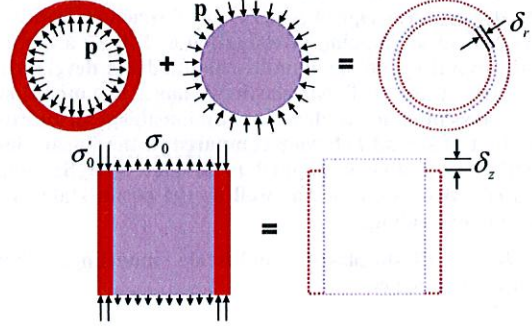


Fig. 4. Decomposition of strand for macro-scale solution.

## III. RRP STRAND MODEL

### A. Model

The multi-scale method described above can be applied to a single strand, as shown in Fig. 3. In this model, the filaments are replaced by a single homogeneous material, whose properties will be determined by an RVE composed of Nb<sub>3</sub>Sn filaments surrounded by copper with bronze cores. This RVE is taken to be a periodic unit cell (PUC).

As a simplification, the homogenized strand is treated as axisymmetric. The reasoning for this treatment is that if the strand is subjected to a change in temperature or an axisymmetric load, the resulting stress inside the core will be uniform, requiring only one RVE to compute the effective behavior. In addition, the Nb<sub>3</sub>Sn is assumed to behave elastically, whereas the copper and bronze are elasto-plastic.

### B. Material Properties

The temperature dependent material properties used for the model are obtained from Mitchell [1]. Since bronze behaves similarly to copper, the properties are taken to be identical.

## IV. TEST CASE: COOLDOWN FROM 300 K TO 4.2 K

### A. Implementation

The macro-scale solution is found by decomposing the inner and outer portions of the strand into two separate problems and then enforcing continuity in the displacements. This process can be seen graphically in Fig. 4, where  $p$  is a radial pressure, and  $\sigma$  is the axial stress.

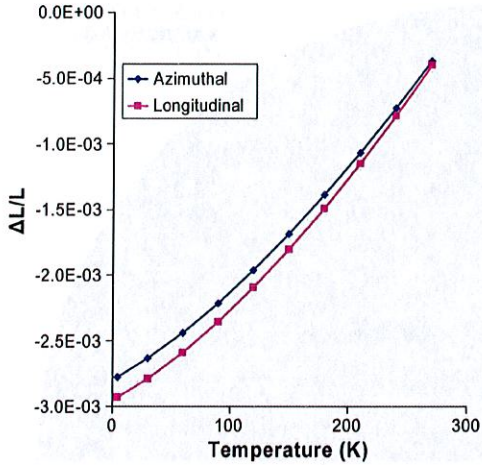


Fig. 5. Thermal strain in a strand due to a cooldown from 300 K to 4.2 K.

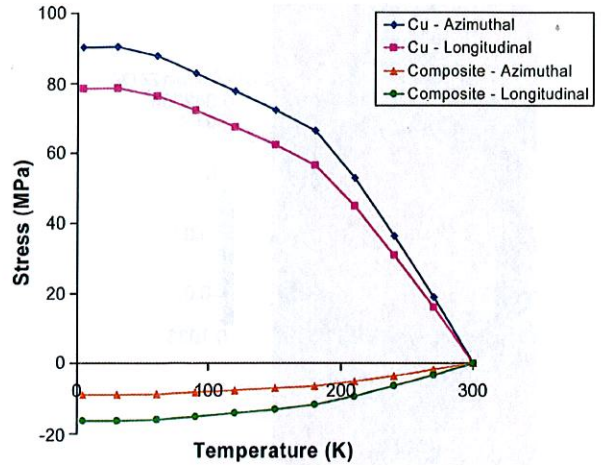


Fig. 6. Average stress in the inner and outer regions of the strand due to a cooldown from 300 K to 4.2 K.

At every loading step, continuity will be enforced by finding the pressures,  $p$  and  $\sigma_0$ , such that the resulting gaps,  $\delta_r$  and  $\delta_z$ , approach zero. This is done numerically using Newton's method

$$\begin{Bmatrix} p^{i+1} \\ \sigma_0^{i+1} \end{Bmatrix} = \begin{Bmatrix} p^i \\ \sigma_0^i \end{Bmatrix} - \begin{bmatrix} \frac{\partial \delta_r}{\partial p} & \frac{\partial \delta_r}{\partial \sigma_0} \\ \frac{\partial \delta_z}{\partial p} & \frac{\partial \delta_z}{\partial \sigma_0} \end{bmatrix}^{-1} \begin{Bmatrix} \delta_r \\ \delta_z \end{Bmatrix}. \quad (2)$$

The stress tensor in the inner region of the strand takes the form

$$\boldsymbol{\sigma}_{inner} = \begin{bmatrix} -p & 0 & 0 \\ 0 & -p & 0 \\ 0 & 0 & \sigma_0 \end{bmatrix} \quad (3)$$

and by enforcing equilibrium in the axial direction and assuming that the outer copper region is thin walled, the corresponding stress tensor is determined to be

$$\boldsymbol{\sigma}_{outer} = \begin{bmatrix} 0 & 0 & 0 \\ 0 & \frac{pR}{t} & 0 \\ 0 & 0 & -\frac{A_{inner}}{A_{outer}}\sigma_0 \end{bmatrix} \quad (4)$$

where  $R$  is the radius of the strand,  $t$  is the thickness, and  $A$  is the cross-sectional area.

The strain in the inner region of the strand is computed by discretizing the RVE into finite elements (see Fig. 3) and numerically calculating the average strain, whereas the strain in the outer region can be determined directly. Plasticity is incorporated by means of a radial return algorithm [5], and deformations are taken to be infinitesimal. Determination of the initial residual stress present will be addressed in future work, and for now it is taken as zero. Ten temperature loading steps are used to bring the strand to 4.2 K. The volume fraction of  $\text{Nb}_3\text{Sn}$  in the RVE is 50%.

## B. Results

The strain and stress in the inner and outer regions of the strand can be seen in Figs. 5 and 6, respectively.

It can be seen that at 4.2 K there is a decrease in length of the strand corresponding to  $-0.293\%$  strain. Similarly, there is a decrease in azimuthal strain, and therefore radial strain, at 4.2 K

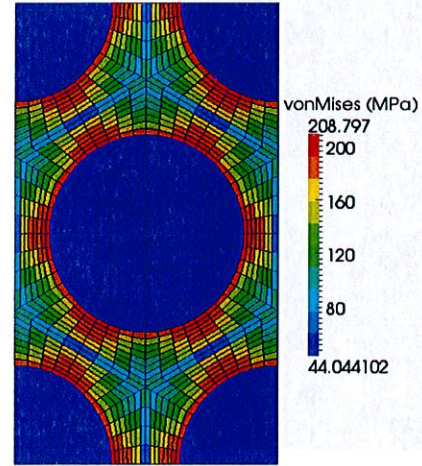


Fig. 7. Von Mises stress in the RVE due to a cooldown from 300 K to 4.2 K.

corresponding to  $-0.277\%$ . These changes in length are noticeably nonlinear, indicating that there is plastic deformation occurring in the outer copper cylinder.

The stress in the outer copper region is tensile, whereas the inner composite experiences an average compressive stress. The average radial and axial stresses in the composite are approximately  $-8.9$  MPa and  $-17.8$  MPa, respectively.

Determination of the stress in the  $\text{Nb}_3\text{Sn}$  filaments can be accomplished by examining the FEM solution of the RVE at 4.2 K. This model uses 8,526 degrees of freedom. The von Mises stress in the RVE is shown in Fig. 7. The magnitude of stress in the individual phases is much larger than the average values calculated at the macro-scale level, with a peak stress of 209 MPa occurring in the  $\text{Nb}_3\text{Sn}$  phase.

The elastic strains in the axial direction inside the RVE are shown in Fig. 8. The copper phase is in tension, whereas the  $\text{Nb}_3\text{Sn}$  experiences an axial compression of  $-0.1\%$ .

The plastic strain in the RVE is shown in Fig. 9. Material flow only occurs in the regions surrounding the filaments. The bronze cores do not deform plastically, however, since they are being loaded hydrostatically.

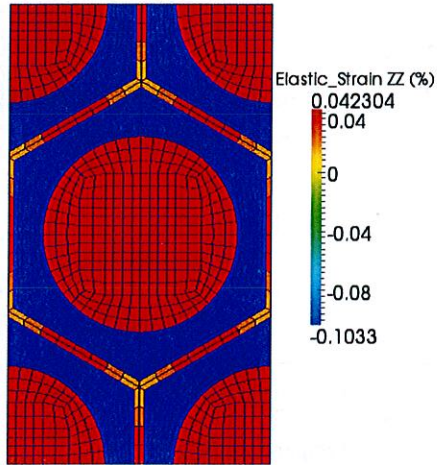


Fig. 8. Elastic axial strain in the RVE due to a cooldown from 300 K to 4.2 K.

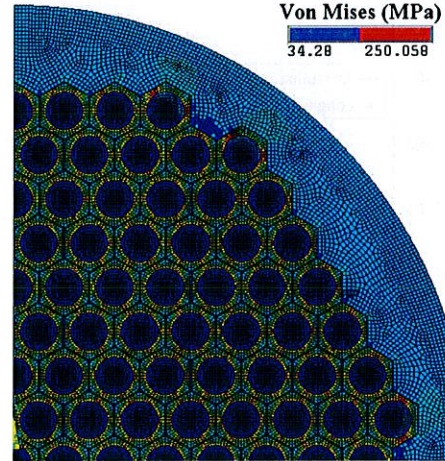


Fig. 10. ANSYS calculation of Von Mises stress in the strand due to a cooldown from 300 K to 4.2 K.

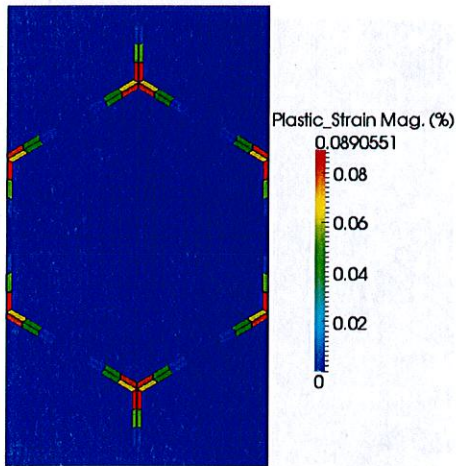


Fig. 9. Plastic strain in the RVE due to a cooldown from 300 K to 4.2 K.

## V. NUMERICAL SIMULATION OF FULL STRAND

In order to gauge the validity of the multiscale model, a cooldown is performed numerically on the fully discretized model of a strand using ANSYS. This model contains 173,382 degrees of freedom, approximately 20 times more than used in the RVE solution. Von Mises stress contours of the strand are shown in Fig. 10.

Although the maximum and minimum values are different than those computed by the multiscale process, these values are located in the outermost filaments. To get an accurate comparison, the inner region of the strand is examined. When the outermost filaments are taken out of consideration, the maximum value of the stress in the  $\text{Nb}_3\text{Sn}$  phase is 208.7 MPa, which is consistent with the solution found using the hierarchical model.

## VI. CONCLUSION

In the present work, a hierarchical model is developed to reduce computational costs associated with resolving microscopic details in a macro-scale problem. Solving a fully resolved strand using ANSYS requires many more degrees of freedom than the multiscale approach, and the difference in computational costs increases as the number of filaments increases. The hierarchical model presented is used to study the behavior between a superconducting strand and its  $\text{Nb}_3\text{Sn}$  filaments. The algorithm produces consistent results with a fully discretized model solved using ANSYS. Possible extensions include utilizing initial residual stresses present in the strand due to heat treatment, the inclusion of voids and cracked filaments, finite deformations, the incorporation of additional length scales, and the inclusion of cases that have a non-uniform stress and strain state; i.e. the loading of Rutherford cables in a magnet. In addition, the use of multiscale modeling to determine the strain state in the  $\text{Nb}_3\text{Sn}$ , and therefore the critical current carrying capacity of the magnet, can be used to optimize magnet design.

## REFERENCES

- [1] N. Mitchell, "Finite element simulations of elasto-plastic processes in  $\text{Nb}_3\text{Sn}$  strands," *Cryogenics*, vol. 45, no. 7, pp. 501–515, 2005.
- [2] D. Boso, M. Lefik, and B. Schrefler, "A multilevel homogenized model for superconducting strands thermomechanics," *Cryogenics*, vol. 45, no. 4, pp. 259–271.
- [3] D. Boso, M. Lefik, and B. Schrefler, "Multiscale analysis of the influence of the triplet helicoidal geometry on the strain state of a  $\text{Nb}_3\text{Sn}$  based strand for ITER coils," *Cryogenics*, vol. 45, no. 9, pp. 589–605.
- [4] D. Arbelaez, "Cable deformation simulation and a hierarchical framework for  $\text{Nb}_3\text{Sn}$  Rutherford cables," *J. Phys.: Conf. Ser.*, vol. 234, p. 02002, 2010.
- [5] J. Simo and R. Taylor, "Consistent tangent operators for rate-independent elastoplasticity," *Comp. Meth. in App. Mech. and Eng.*, vol. 48, no. 1, pp. 101–118, 1985.